

Distortion of the Wigner distribution by a Coulomb interaction

Author: Elena Seara, eseararo29@alumnes.ub.edu

Facultat de Física, Universitat de Barcelona, Diagonal 645, 08028 Barcelona, Spain.

Advisor: Miguel Ángel Escobedo, miguel.a.escobedo@fqa.ub.edu

Abstract: The goal of this work is to study the distortion of the Wigner function of a heavy quark interacting by a Coulomb potential in a quark gluon plasma. To carry it out, we programmed a model using FORTRAN 77 that integrates the Wigner function for a Coulomb wave function. With that we want to test if the approximation of using a free particle wave function to calculate the Wigner function of the unbound particles in the Coalescence model is a good approximation.

Keywords: Wigner distribution, quark gluon plasma, charmonium, Coalescence model.

SDGs: 4. Quality education, 8. Decent work and economic growth.

I. INTRODUCTION

It is believed that in the early stages of the universe, it existed a form of matter called Quark-Gluon plasma (QGP), a hot and dense fluid where quarks and gluons are not confined inside hadrons. Nowadays, through experiments such as ALICE or RHIC, we are able to recreate the quark-gluon plasma by high-energy nuclear collisions. Unlike other particles such as electrons, quarks are found confined, forming bound states in the form of hadrons. Only in specific conditions of temperature and density, we can observe unbound quarks and gluons.

In the standard model, QCD is the theory that explains strong interaction. QCD considers that every quark and gluon has a color charge, there are three different possible color states. On one hand, quarks have mass and electric charge while gluons don't. Gluons, on the other hand, play a very important role being the mediators of strong interactions, allowing quarks to change between different color states during interactions. Only states with a singlet state of color are observable; this is called color confinement. Thus for mesons, the only possibility for observable states is a color-anticolor state. Color confinement implies that quarks as well as gluons cannot be observed as free unbound particles, they have to be bound in order to have a global color charge equal to 0.

It is interesting to study heavy quarks produced in heavy ion collision because, as studies show, they are all produced at the early stages of the collisions [1], since more energy is needed to produce them due to their mass, and "their abundances remain essentially frozen for the entire duration of the collisions" [2], serving us as a probe to characterize the QGP. In this work we are going to focus in the study of $c\bar{c}$ since they are more abundant as products of said collisions. b and \bar{b} have larger masses than c and \bar{c} , ($m_{c,\bar{c}} = 1.5\text{GeV}$, $m_{b,\bar{b}} = 4.2\text{GeV}$) [3], it is for that reason that they require more energy to be produced and so they are produced with less frequency.

In the same way, we are going to discard t, \bar{t} states since they are greatly unstable.

In heavy ion collision, when the two heavy ions first collide at ultra-relativistic velocities, particles quickly interact releasing great quantities of energy in a reduced volume which produces high temperatures and densities, at certain values of temperature and density we can see a phase transition in which a new state of matter is formed. Said conditions enable quarks and gluons to be unconfined from nucleons thus forming this new state of matter, QGP. In this context, the formation of bound states of $c\bar{c}$, such as J/ψ , can be impaired by the screening of the binding force due to high temperature and density of the QGP, this phenomenon is called suppression. Suppression of J/ψ can also happen due to collisions with particles from the plasma as stated in [2]. The opposite can also happen, at temperatures above the phase transition temperature, recombination of quarks and gluons into hadrons can occur.

We can calculate the number of states that recombine in each instant of time using the coalescence model [4]. Since small relative distances and momenta are necessary for the recombination of quarks, coalescence models are developed in phase space. The mathematical tool used to work in phase space is the Wigner function. In the coalescence model the probability to form bound states is proportional to the convolution of the Wigner function of the bound state and the Wigner function that correspond to the distribution of the N particles that form the bound state [5]. It is very common to approximate the Wigner function of the distribution of the N particles, in our case 2 quarks, to the product of the Wigner function of every particle that forms the bound state, thus assuming independent quarks. In our work we want to test if assuming free independent particles for the non-bounded state is a good approximation.

As stated in [5], we can calculate the probability distribution as a function of p_t (momentum of the particles that are formed in the perpendicular direction to the par-

ticle beams of the ion collision) of the formed mesons as follows:

$$\frac{d^2 P_\Psi}{dp_T^2} = g_\Psi \int \prod_{i=1}^2 \frac{d^3 r_i d^3 p_i}{(2\pi\hbar)^3 E_i} W_q(r_1, p_1) W_{\bar{q}}(r_2, p_2) \times W_\Psi(r_1, p_1; r_2, p_2) \delta(p_T - p_{1,T} - p_{2,T}) \quad (1)$$

W_q , $W_{\bar{q}}$ and W_Ψ are the Wigner functions of the quark, antiquark and the recombined meson respectively, p_i and r_i are the momentum and spatial coordinates, and g_Ψ is a probability factor of forming a white meson.

Coulomb interaction in a QGP arises from QCD's asymptotic freedom, which states that at shorter distances, interaction between particles is weaker than at longer distances, therefore, as stated in [5], "at short interquark distances, the interaction is dominated by one-gluon exchange and we might expect a Coulomb-like potential". It is shown that the potential for $r \leq 0.1 fm$ is given by:

$$V(r) = -\frac{4}{3} \frac{\alpha_s}{r} \quad (2)$$

Where α_s is the strong coupling constant which indicates the strength of the interaction, and $\frac{4}{3}$ is the factor of color C for a singlet state. Although α_s increases with r , for our study, we can neglect this variation and take α_s constant and equal to 0.5.

In a thermal distribution, all directions are equally probable, therefore the Wigner function of free unbound quarks in this regime can be calculated using s-waves, wave functions corresponding to angular momentum equal to 0, which only depend on the radius.

For this work we are going to make a set of assumptions:

1. We are going to work at constant temperature although "local thermalization of the system created in heavy ion collision is yet to be tested" [6].
2. We are going to take the non-relativistic approach since the rest mass of $c\bar{c}$ is larger than the typical kinetic energy.

In section II we are going to state the principles of the Wigner function. In section III, we are going to calculate the Wigner function of an s-wave free particle. With that, and calculating the Wigner function of the Coulomb wave function, we are going to study the distortion of the Wigner function by a Coulomb potential. In section IV we are going to comment the results obtained in the previous section. The code used for the numerical calculations will appear in the appendix A.

II. PRINCIPLES OF THE WIGNER FUNCTION

As stated in [7] "The Wigner function is a phase space description of the density operator, which in turn represents a quantum state."

The Wigner function is a real function that takes real values of position and momentum. It holds all the information of the quantum state contained in the density matrix.

The Wigner function is a pseudo probability since it can take negative values. Although we can't directly interpret the regions where the Wigner distribution is negative since it is not clear what a "negative probability" would mean [7]; we know that those regions indicate that the system behaves purely quantum and it cannot be described classically.

The Wigner distribution can be calculated as follows:

$$W(\vec{r}, \vec{p}) = \int_{-\infty}^{\infty} e^{i\vec{\xi} \cdot \vec{p}} \langle \vec{r} + \frac{1}{2}\vec{\xi} | \hat{\rho} | \vec{r} - \frac{1}{2}\vec{\xi} \rangle d\vec{\xi} \quad (3)$$

We arrive to this result by taking the normalized Fourier Transform of the element matrix $\langle \vec{r} + \frac{1}{2}\vec{\xi} | \hat{\rho} | \vec{r} - \frac{1}{2}\vec{\xi} \rangle$ that describes the jump from the position eigenstate $\langle \vec{r}_+ |$ to the position eigenstate $|\vec{r}_- \rangle$, where $\hat{\rho}$ is the density matrix of the c, \bar{c} and \vec{r} is the position vector, and $\vec{\xi}$ is the conjugate of the momentum and the variable over which we are integrating.

Note that if we integrate over all p , we get by construction the probability distribution of r . The same holds if we integrate over all r , we get the probability distribution of p .

The above result is the Wigner function for a mixed state. In this work we are going to study only pure states. For a pure state, the density operator is defined as:

$$\hat{\rho} = |\psi\rangle\langle\psi| \quad (4)$$

Substituting in equation (3), we obtain:

$$W(\vec{r}, \vec{p}) = \int_{-\infty}^{\infty} e^{-i\vec{p}\vec{\xi}/\hbar} \left\langle \vec{r} + \frac{1}{2}\vec{\xi} \left| \psi \right\rangle \left\langle \psi \left| \vec{r} - \frac{1}{2}\vec{\xi} \right\rangle d\vec{\xi} \quad (5)$$

$$= \int_{-\infty}^{\infty} e^{-i\vec{p}\vec{\xi}/\hbar} \psi\left(\vec{r} + \frac{1}{2}\vec{\xi}\right) \psi^*\left(\vec{r} - \frac{1}{2}\vec{\xi}\right) d\vec{\xi} \quad (6)$$

This equation provides a phase space description of an arbitrary state ψ [7].

III. INTEGRATING THE WIGNER DISTRIBUTION

To integrate the Wigner distribution we programmed a Monte Carlo method in FORTRAN 77 in which we have done the calculations in spherical coordinates, where we have chosen a random uniformly distribution for $\vec{\xi}$ ($\vec{\xi}$ is the conjugate of the momentum). We have calculated for $\vec{r} \parallel \vec{p}$:

$$r_{\parallel}^{\pm} \equiv |\vec{r} \pm \frac{1}{2}\vec{\xi}| = \sqrt{r^2 + \frac{\xi^2}{4} \pm r\xi \cos \theta} \quad (7)$$

And for $\vec{r} \perp \vec{p}$:

$$r_{\perp}^{\pm} \equiv |\vec{r} \pm \frac{1}{2}\vec{\xi}| = \sqrt{r^2 + \frac{\xi^2}{4} \pm r\xi \sin \theta \sin \phi} \quad (8)$$

Where $\vec{\xi} = (\xi \sin \theta \cos \phi, \xi \sin \theta \sin \phi, r \cos \theta)$.

To calculate the distortion of the Wigner function by a Coulomb potential, first we note that the wave function of a plane wave is:

$$\psi_{\vec{p}_0}(\vec{r}) = \frac{1}{(2\pi)^{3/2}} e^{i\vec{p}_0 \vec{r}} \quad (9)$$

To project it on a s-wave:

$$\begin{aligned} \psi_{P_0}^s(r) &= Y_{00}(\Omega) \int d\Omega' \psi_{\vec{p}_0}(\vec{r}) Y_{00}(\Omega') \\ &= \frac{2\pi}{4\pi(2\pi)^{3/2}} \int_0^\pi d\theta \sin \theta e^{ip_0 r \cos \theta} \\ &= \frac{1}{(2\pi)^{3/2}} \frac{\sin(p_0 r)}{p_0 r} \end{aligned} \quad (10)$$

Now for the Coulomb wave function we have:

$$\psi(r) = N \frac{u_E(\sqrt{2\mu E}r)}{\sqrt{4\pi r}} \quad (11)$$

Where we have calculated u_E with the subroutine COUL90 from [7] and N is a normalization constant.

We have chosen N so that for large r , the coulomb wavefunction resembles the s-wavefunction of a free particle. Note that:

$$\lim_{\rho \rightarrow \infty} u_E(\rho) \sim \sin \left(\rho - \sqrt{\frac{\mu \alpha^2}{2E}} \log(2\rho) + \arg \left(1 + i\sqrt{\frac{\mu \alpha^2}{2E}} \right) \right) \quad (12)$$

Using the normalization convention from [8]:

$$\psi(r) = \sqrt{\frac{\mu}{2\pi^2 \sqrt{2\mu E}}} \frac{u_E(\sqrt{2\mu E}r)}{r} \quad (13)$$

Substituting in the Wigner function:

$$W_{p_0}^C(r, p) = \frac{\mu}{2\pi^2 p_0} \int d\xi^3 e^{-i\vec{p}\vec{\xi}} \frac{u_E(p_0 r^+)}{r^+} \frac{u_E(p_0 r^-)}{r^-} \quad (14)$$

Where p_0 corresponds to the chosen energy and we calculate for r^+ and r^- parallel and perpendicular.

This integral is very difficult to calculate since the integrand oscillates very quickly for large r^{\pm} . We can fix this by subtracting the oscillating part which we can calculate analytically. So if we note that from eq. (12), $\sin(\rho)$ is the radial s-wavefunction of a free particle, we obtain:

$$\begin{aligned} W_{p_0}^C(r, p) &= \frac{\mu}{2\pi^2 p_0} \int d\xi^3 e^{-i\vec{p}\vec{\xi}} \\ &\times \left(\frac{u_E(p_0 r^+)}{r^+} \frac{u_E(p_0 r^-)}{r^-} - \frac{\sin(p_0 r^+)}{r^+} \frac{\sin(p_0 r^-)}{r^-} \right) \\ &+ W_{free} \end{aligned} \quad (15)$$

Where W_{free} is equation (50) of [8]:

$$W_{free} = \frac{2pr^2 \sin \theta}{\pi p_0} J_0 \left(2\sqrt{p^2 - p_0^2} r \sin \theta \right) \quad (16)$$

Here θ is the angle between \vec{r} and \vec{p} , and J_0 denotes the Bessel function of order 0. This equation vanishes when $\theta = 0$ and $\theta = \pi$, i.e. when \vec{r} and \vec{p} are parallel or antiparallel (angular momentum equal to 0). It also vanishes if $p > p_0$. Equation (16) reaches a maximum for $p = p_0$.

IV. RESULTS

We expect to see a better approximation for high energies since in that case, the influence of the Coulomb potential is negligible compared to the energy of the quark. Therefore, for the high energy regime, we expect the distortion of the Wigner function to go to 0 so that we can approximate the quark in a Coulomb potential for a free quark, thus replace the wavefunction of the quark to that of a free state.

We also expect to see the Wigner function we have calculated go to 0 for large r since by construction, the Coulomb wave function approximates to the s-wave projection of a plane wave for large r , as we have seen in equation (12).

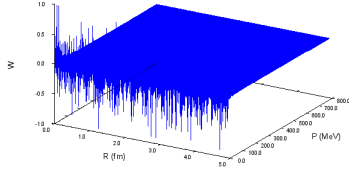


FIG. 1: Distortion of the Wigner function for $E = 200 \text{ MeV}$ and $\vec{r} \parallel \vec{p}$.

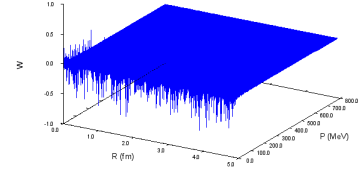


FIG. 5: Distortion of the Wigner function for $E = 1000 \text{ MeV}$ and $\vec{r} \perp \vec{p}$.

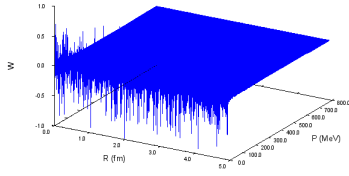


FIG. 2: Distortion of the Wigner function for $E = 200 \text{ MeV}$ and $\vec{r} \perp \vec{p}$.

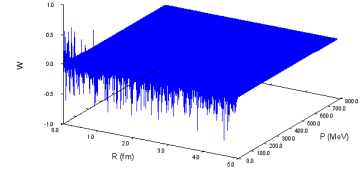


FIG. 6: Distortion of the Wigner function for $E = 1000 \text{ MeV}$ and $\vec{r} \parallel \vec{p}$.

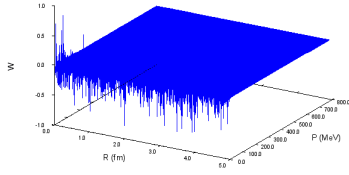


FIG. 3: Distortion of the Wigner function for $E = 600 \text{ MeV}$ and $\vec{r} \parallel \vec{p}$.

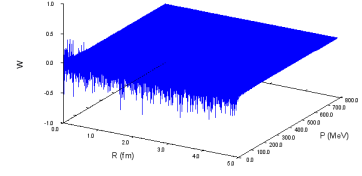


FIG. 7: Distortion of the Wigner function for $E = 2000 \text{ MeV}$ and $\vec{r} \parallel \vec{p}$.

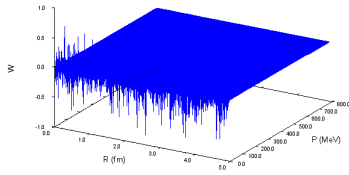


FIG. 4: Distortion of the Wigner function for $E = 600 \text{ MeV}$ and $\vec{r} \perp \vec{p}$.

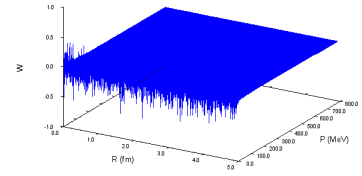


FIG. 8: Distortion of the Wigner function for $E = 2000 \text{ MeV}$ and $\vec{r} \perp \vec{p}$.

For both $\vec{r} \perp \vec{p}$ and $\vec{r} \parallel \vec{p}$ the expected results show. We can see very similar figures for both cases, for small

r and p the modification of the Wigner function is considerable, and for the rest it goes to 0. We can also see that the distortion of the Wigner function decreases as energy increases. For small r and p the graphs look very oscillating, This is due to the lack of precision of the implemented method. In these regions of the graphs it is most likely that if we took the absolute value it would be close to zero since the distortion of the Wigner function is oscillating around it. We cannot see this because of the commented lack of precision.

V. CONCLUSION

We have studied how the Wigner function is distorted by a Coulomb potential in order to tell if we can approximate the Wigner function of the N unbound states used in the Coalescence model to N Wigner functions of a free s-wave. With the calculations we have done we can conclude that for large r and p the approximation holds. For small r and p , the Monte Carlo method used to integrate does not allow us to get to the wanted precision,

as we can see in the figures. This is because the functions we are integrating are very oscillating, therefore, other methods such as the Fast Fourier Transform, could be more suitable. However, the size of the modifications obtained indicate large modifications in the region relevant for charmonium physics. Note that the typical value of the radius of a bound state of charmonium is $0.5 fm$ and its typical momentum is $400 MeV$. In summary, although the Monte Carlo integration did not achieve the level of accuracy that we expected, we have obtained indications that the inclusion of the Coulomb potential might be needed to obtain accurate predictions for recombination with the coalescence model.

Acknowledgments

I want to thank my tutor, Miguel Ángel Escobedo, for his help and guidance. I'm especially grateful to my family for their continued support.

-
- [1] J. Adams *et al.* [STAR Collaboration], Phys. Rev. Lett. **94**, 062301 (2005); Y.F. Zhang, **nuc1-ex/0607711**.
 - [2] S. Navas *et al.* (Particle Data Group), Phys. Rev. D **110**, 030001 (2024).
 - [3] Jean-Paul Blaizot, Davide De Boni, Pietro Faccioli, Giovanni Garberoglio, "Heavy quark bound states in a quark-gluon plasma: Dissociation and recombination", *Nuclear Physics A*, **946**, 2016.
 - [4] V. Greco, C. M. Ko, R. Rapp, "Quark coalescence for charmed mesons in ultrarelativistic heavy-ion collisions," *Physics Letters B*, vol. 595, issues 1–4, pp. 202–208, 2004. doi:10.1016/j.physletb.2004.06.064. <https://www.sciencedirect.com/science/article/pii/S0370269304009037>
 - [5] Neil Lindsey, "Path Integral Calculation of the Wigner Function", figshare, <https://hdl.handle.net/2134/24509> (2019).
 - [6] Li Yan, Pengfei Zhuang, Nu Xu, "J/ Production in Quark-Gluon Plasma", Phys. Rev. Lett. **97**, 232301 (2006), doi: 10.1103/PhysRevLett.97.232301.
 - [7] A.R. Barnett, "The Calculation of Spherical Bessel Functions and Coulomb Functions", <https://fresco.org.uk/programs/barnett/APP23.pdf>.
 - [8] J. P. Dahl, S. Varro, A. Wolf, W. P. Schleich, "Wigner functions of s waves", *Phys. Rev. A* **75**, 052107 (2007), doi:10.1103/PhysRevA.75.052107.

Distorsió de la distribució de Wigner per una interacció de Coulomb

Author: Elena Seara, eseararo29@alumnes.ub.edu

Facultat de Física, Universitat de Barcelona, Diagonal 645, 08028 Barcelona, Spain.

Advisor: Miguel Ángel Escobedo, miguel.a.escobedo@fqa.ub.edu

Resum: L'objectiu d'aquest treball és estudiar la distorsió de la funció de Wigner d'un quark pesat que interactua mitjançant un potencial de Coulomb en un plasma de quarks i gluons. Per dur-ho a terme, hem programat un model utilitzant FORTRAN 77 que integra la funció de Wigner per a una funció d'ona de Coulomb. Amb això volem veure si fer l'aproximació d'utilitzar una funció d'ona d'una partícula lliure per calcular la funció de Wigner de les partícules no lligades en el model de coalescència és una bona aproximació.

Paraules clau: Distribució de Wigner, plasma de quarks i gluons, charmonium, model de Coalescència.

ODSs: 4. Educació de qualitat, 8. Treball digne i creixement econòmic.

Objectius de Desenvolupament Sostenible (ODSs o SDGs)

1. Fi de la es desigualtats	10. Reducció de les desigualtats	
2. Fam zero	11. Ciutats i comunitats sostenibles	
3. Salut i benestar	12. Consum i producció responsables	
4. Educació de qualitat	X 13. Acció climàtica	
5. Igualtat de gènere	14. Vida submarina	
6. Aigua neta i sanejament	15. Vida terrestre	
7. Energia neta i sostenible	16. Pau, justícia i institucions sòlides	
8. Treball digne i creixement econòmic	X 17. Aliança pels objectius	
9. Indústria, innovació, infraestructures		

Aquest TFG, part d'un grau universitari de Física, es relaciona amb l'ODS 4, en particular amb la fita 4.4 perquè contribueix a l'educació universitària. També es relaciona amb l'ODS 8, en particular amb la fita 8.2 ja que contribueix a la modernització tecnològica.

ABSTRACT GRÀFIC

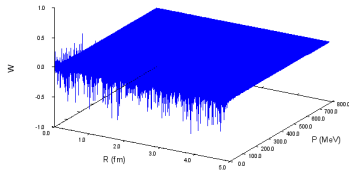


FIG. 9: Distorsió de la funció de Wigner per $E = 1000 \text{ MeV}$ i $\vec{r} \perp \vec{p}$.

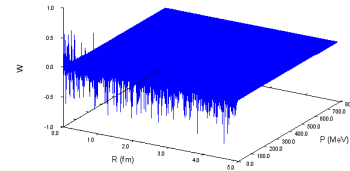


FIG. 10: Distorsió de la funció de Wigner per $E = 1000 \text{ MeV}$ i $\vec{r} \parallel \vec{p}$.

Appendix A: Code

```

PROGRAM TFG
IMPLICIT NONE
DOUBLE PRECISION XSI(100),THETA(100),PHI(100),HP,HR,CTEPL
DOUBLE PRECISION R, P, INT, ERROR, INTPERP,PMIN, RMIN, PCERO
DOUBLE PRECISION PI,MASSAR,G(100), RMAX,F(100),PMAX
DOUBLE PRECISION FC(100), GC(100), FCP(100), GCP(100), E
DOUBLE PRECISION FPL(100), FPP(100), A0, PAU
INTEGER N, I, L, M, J, ISEED, K, IFAIL
COMMON/DADES/PI, MASSAR, N
EXTERNAL RMPARALLEL, RMPERPENDICULAR

```

```

ISEED=20447725
CALL SRAND(ISEED)

```

```

PI=4.D0*DATAN(1.D0)
MASSAR=1549.D0
N=100

```

```

PMAX=800.D0
PMIN=0.D0
RMIN=0.D0/PMAX
RMAX=0.025D0
E=200.D0
PCERO=DSQRT(2.D0*MASSAR*E)
L=0
M=0

```

```

HR=(RMAX-RMIN)/DBLE(N)
HP=(PMAX-PMIN)/DBLE(N)

```

```

CALL VUNIFORME(XSI, THETA, PHI, 0.025D0)

```

```

OPEN(1, FILE="COULOMB_PARALLEL_1.DAT")
DO I=1, N
  DO J=1, N
    R=RMIN+(I*HR)
    P=PMIN+(J*HP)
    CALL PARALLEL(XSI, THETA, PHI, E, R, P, F)
    INT=0.D0
    DO K=1, N
      INT=INT+(F(K))
    ENDDO
    INT=2.D0*1970.D0*PI*PI*INT/(N*P)
    WRITE(1,*)R*197.D0, P, INT
  ENDDO
  WRITE(1,*)
ENDDO
CLOSE(1)
OPEN(2, FILE="COULOMB_PERP_1.DAT")
DO I=1, N
  DO J=1, N
    R=RMIN+(I*HR)
    P=PMIN+(J*HP)
    CALL PERPENDICULAR(XSI, THETA, PHI, E, R, P, F)
    INT=0.D0
    DO K=1, N
      INT=INT+(F(K))
    ENDDO
    INT=2.D0*1970.D0*PI*PI*INT/(N*P)
    WRITE(2,*)R*197.D0, P, INT
  ENDDO
  WRITE(2,*)
ENDDO
CLOSE(2)

```

```

END PROGRAM TFG

```

```

SUBROUTINE VUNIFORME(XSI, THETA, PHI, LIM)
IMPLICIT NONE
DOUBLE PRECISION XSI(N), THETA(N), PHI(N), PI, MASSAR, LIM
INTEGER N, I
COMMON/DADES/PI, MASSAR, N

```

```

DO I=1, N
  XSI(I)=(LIM*RAND())
  THETA(I)=PI*RAND()
  PHI(I)=2.D0*PI*RAND()
ENDDO
RETURN
END

```

```

C CALCULA EL MODULO DE R+XSI/2=RMA Y R-XSI/2=RME PARA P Y R PARALELOS
SUBROUTINE RMPARALLEL(XSI, THETA, R, RMA, RME)
IMPLICIT NONE
DOUBLE PRECISION XSI(N), R, RMA(N), RME(N), PI, THETA(N), A
DOUBLE PRECISION MASSAR
INTEGER I, N
COMMON/DADES/PI, MASSAR, N

```

```

DO I=1, N
  A=DCOS(THETA(I))
  RMA(I)=DSQRT((R**2)+(XSI(I)*0.5D0)**2)+(R*XSI(I)*A))
  RME(I)=DSQRT((R**2)+(XSI(I)*0.5D0)**2)-(R*XSI(I)*A))
ENDDO

```

```

RETURN
END SUBROUTINE

```

```

C CALCULA LA FUNCION A INTEGRAR PARA R Y P PARALELOS
C N: DIMENSION DE LOS ARRAYS
C RMA Y RME: ARRAYS R+ Y R_
C Y: ARRAY CON AS
C ETAP: CONSTANTE DE SOMMERFELD, ALPHAS CTE DE INTERACCION FIUERTE
SUBROUTINE PARALLEL(XSI, THETA, PHI, E, R, P, F)
IMPLICIT NONE
DOUBLE PRECISION BRA(N), XB, FC(1), GC(1), FCP(1), GCP(1)
DOUBLE PRECISION Y(N), KET(N), RME(N), XK, THETA(N), XSI(N), R, P
DOUBLE PRECISION K, CTE, T, PI, RMA(N), ALPHAS, F(N), PHI(N)
DOUBLE PRECISION MASSAR, ETAP, E, A(N), B(N), C(N), D(N)
INTEGER IFAIL, I, N
COMMON/DADES/PI, MASSAR, N

```

```

CALL VUNIFORME(XSI, THETA, PHI, 10.D0/P)
CALL RMPARALLEL(XSI, THETA, R, RMA, RME)
ETAP=MASSAR*0.5D0/(DSQRT(E*2.D0*MASSAR))
K=DSQRT(2.D0*MASSAR*E)

```

```

C PSI PARA R+
DO I=1, N
  XB=RMA(I)*K
  CALL COUL90(XB, ETAP, 0.D0, 0, FC, GC, FCP, GCP, 0, IFAIL)
  BRA(I)=FC(1)/RMA(I)
ENDDO
C PSI PARA R_
DO I=1, N
  XK=RME(I)*K
  CALL COUL90(XK, ETAP, 0.D0, 0, FC, GC, FCP, GCP, 0, IFAIL)
  KET(I)=FC(1)/RME(I)
ENDDO

```

```

DO I=1, N
  A(I)=MASSAR/(2.D0*(PI**2)*K)*DCOS(P*XSI(I)*DCOS(THETA(I)))
  B(I)=DSIN(THETA(I))*(XSI(I)**2)
  D(I)=(BRA(I)*KET(I))
  C(I)=(DSIN(K*RMA(I))*DSIN(K*RME(I)))/(RMA(I)*RME(I))
  F(I)=(A(I)*B(I)*(D(I)-C(I)))

```

```

ENDDO

```

```

RETURN
END SUBROUTINE

```

```

C CALCULA EL MODULO DE R+XSI/2=RMA Y R-XSI/2=RME PARA P Y R PERPEDICUALES
SUBROUTINE RMPERPENDICULAR(XSI, THETA, PHI, R, RMA, RME)
IMPLICIT NONE
DOUBLE PRECISION XSI(N), R, RMA(N), RME(N), PI, THETA(N), A
DOUBLE PRECISION MASSAR, PHI(N)

```

```

      INTEGER I, N
      COMMON/DADES/PI, MASSAR, N

      DO I=1, N
        A=DSIN(THETA(I))*DSIN(PHI(I))
        RMA(I)=DSQRT((R**2)+(XSI(I)*0.5D0)**2)+(R*XSI(I)*A))
        RME(I)=DSQRT((R**2)+(XSI(I)*0.5D0)**2)-(R*XSI(I)*A))
      ENDDO

      RETURN
      END SUBROUTINE

C CALCULA LA FUNCION A INTEGRAR PARA R Y P PARALELOS
C N: DIMENSION DE LOS ARRAYS
C RMA Y RME: ARRAYS R+ Y R-
C Y: ARRAY CON AS
C ETAP: CONSTANTE DE SOMMERFELD, ALPHAS CTE DE INTERACCION FIUERTE
      SUBROUTINE PERPENDICULAR(XSI, THETA, PHI, E, R, P, F)
      IMPLICIT NONE
      DOUBLE PRECISION BRA(N), XB, FC(1), GC(1), FCP(1), GCP(1)
      DOUBLE PRECISION Y(N), KET(N), RME(N), XK, THETA(N), XSI(N), R, P
      DOUBLE PRECISION K, CTE, T, PI, RMA(N), ALPHAS, F(N), PHI(N), ETAW
      DOUBLE PRECISION MASSAR, ETAP, E, WL(N), RW, A(N), B(N), C(N), D(N)
      INTEGER IFAIL, I, N
      COMMON/DADES/PI, MASSAR, N

      CALL VUNIFORME(XSI, THETA, PHI, 10.D0/P)
      CALL RMPERPENDICULAR(XSI, THETA, PHI, R, RMA, RME)
      ETAP=MASSAR*0.5D0/(DSQRT(E*2.D0*MASSAR))
      K=DSQRT(2.D0*MASSAR*E)

C PSI PARA R+
      DO I=1, N
        XB=RMA(I)*K
        CALL COUL90(XB, ETAP, 0.D0, 0, FC, GC, FCP, GCP, 0, IFAIL)
        BRA(I)=FC(1)/RMA(I)
      ENDDO

C PSI PARA R-
      DO I=1, N
        XK=RME(I)*K
        CALL COUL90(XK, ETAP, 0.D0, 0, FC, GC, FCP, GCP, 0, IFAIL)
        KET(I)=FC(1)/RME(I)
      ENDDO

      RW=2.D0*DSQRT(K**2-P**2)*R
      ETAW=0.D0
      CALL COUL90(RW, ETAW, 0.D0, 0, FC, GC, FCP, GCP, 0, IFAIL)
      DO I=1, N
        WL(I)=(2.D0/(K*PI))*P*(R**2)*FC(1)
      ENDDO

      DO I=1, N
        A(I)=MASSAR/(2.D0*(PI**2)*K)*DCOS(P*XSI(I)*DCOS(PHI(I)))
        B(I)=DSIN(THETA(I))*(XSI(I)**2)
        D(I)=(BRA(I)*KET(I))
        C(I)=(DSIN(K*RMA(I))*DSIN(K*RME(I)))/(RMA(I)*RME(I))
        F(I)=(A(I)*B(I)*(D(I)-C(I)))+WL(I)
      ENDDO

      RETURN
      END SUBROUTINE

```